ISBN: 978-3-95450-179-3 doi:10.18429/JACoW-FEL2017-TUP002

NUMERICAL STUDIES ON RF-INDUCED TRAJECTORY VARIATIONS AT THE EUROPEAN XFEL

T. Hellert, B. Beutner, N. Walker, W. Decking, DESY, Hamburg, Germany

Abstract

At the European X-Ray Free-Electron-Laser, superconducting TESLA-type cavities are used for acceleration of the driving electron bunches. Due to the high achievable duty cycle, a long radio frequency (RF) pulse structure can be provided, which allows to operate the machine with long bunch trains. The required pointing stability of the FEL radiation places stringent restrictions on the acceptable trajectory variations of individual electron bunches. Therefore a transverse intra-bunch-train feedback system (IBFB) is located upstream of the undulator section. However, intra-bunch-train variations of RF parameters and misalignments of RF structures induce significant trajectory variations that may exceed the capability of the IBFB. In this paper we give an estimate of the expected RF induced intra-bunch-train trajectory variation for different machine realizations and investigate on methods for their limitation.

INTRODUCTION

The European X-Ray Free-Electron Laser (EuXFEL) Facility [1–3] is built in Hamburg and is currently undergoing commissioning [4]. It will provide FEL radiation with wavelengths from 0.05 nm to 5 nm. Acceleration of the driving electron bunches is achieved by using superconducting TESLA-type [5] cavities. The long RF pulse structure allows to provide long bunch-trains adapted to the needs of the experiments. Up to 2700 bunches are accelerated within one RF pulse with a pulse repetition rate of 10 Hz and a bunch spacing down to 222 ns, thus 27000 bunches per second can be used for the experiments.

The designated pointing stability of the photon beam leads to a stability requirement of 3 µm maximum trajectory spread within one bunch-train in the undulator section. A conservative estimate predicts worst case beam trajectory perturbations, e.g. from magnet vibrations or spurious dispersion, of about ±100 µm assuming a beta function of 30 m [6]. This magnitude of amplitude can be corrected for individual bunches at the entrance to the undulator section by the transverse intra-bunch-train feedback system (IBFB) [7]. However, RF-induced trajectory variations have not been considered in the design studies of the IBFB.

At EuXFEL, several cavities with individual operational limits [8] are supplied by one RF power source. Within the bunch-train, the low-level-RF system (LLRF) [9, 10] is able to restrict the variation of the vector sum of the accelerating gradient of one RF station sufficiently [11]. However, individual cavities have an intrinsic variation of RF parameters within one bunch train, caused by the effects of beam loading and Lorentz force detuning [12]. Misaligned cavities in combination with variable RF parameters induce intra-bunch-train trajectory variations [12]. Coupler kick variations caused by variations of the detuning are additional beam dynamics perturbations within one bunch train. In this paper we investigate their magnitude for different machine realizations and present methods for their limitation.

MODEL SETUP

A detailed description of the utilized beam dynamics model can be found in Ref. [12]. We use a combination of axially symmetric beam transport matrices [13] and discretized coupler kicks [14]. Misalignments are modeled by coordinate system transformations. The EuXFEL linear accelerator increases the electron beam energy up to 17.5 GeV in three separate sections: L1, L2 and L3, each consisting out of 4, 12 and 84 accelerating modules, respectively. Each module contains eight cavities and a quadrupole magnet, providing a FODO lattice in the accelerating sections. Initial beam energy is 150 MeV for L1, 600 MeV for L2 and 2.4 GeV for L3. If not stated differently, for each machine seed the following model parameters are randomly created within their range: variation of amplitude $\Delta V = 2\,\mathrm{MV\,m^{-1}}$ and phase $\Delta\phi = 4°$ of the accelerating field and the detuning $\Delta f = 20\,\mathrm{Hz}$ of individual cavities within the bunch train. Furthermore the offset $\Delta u_{\mathrm{cav}} = 0.5\,\mathrm{mm}$ and tilt $\Delta u'_{\mathrm{cav}} = 0.25\,\mathrm{mrad}$ of cavities and modules, $\Delta u_{\mathrm{mod}} = 0.5\,\mathrm{mm}$ and $\Delta u'_{\mathrm{mod}} = 0.2\,\mathrm{mrad}$, respectively. The above values are expected for nominal machine operation.

BEAM DYNAMICS SIMULATIONS

Before conducting a statistical analysis of each accelerating section, tracking results of one random machine realization are presented. Figure 1 shows the intra-bunch-train trajectory variation for the horizontal and vertical plane as it could be recorded at the beam position monitors at each module at EuXFEL. Mean bunch train offsets are subtracted. The lower row of Figure 1 additionally shows the normalized trajectory variation $\Delta\tilde{u}$. It will be defined as the maximum possible offset variation at a point with zero divergence and $\beta_u = 30\,\mathrm{m}$, where u stands for x and y, respectively. The normalized trajectory variation evolves non-monotonically throughout the machine. The correlation of particular misalignments of cavities and their RF parameters can affect the initial trajectory variation at the entrance of the cavity constructively or destructively. An accurate consideration must involve statistical methods.

The accumulated normalized intra-bunch-train trajectory variation $\Delta\tilde{u}$ is calculated for L1, L2 and L3 independently. 10^5 random sets of misalignments and RF parameters are evaluated. Figure 2 shows a histogram of $\Delta\tilde{u}$, as induced in each linac. Critical trajectory variation is defined as the

ISBN: 978-3-95450-179-3 doi:10.18429/JACoW-FEL2017-TUP002

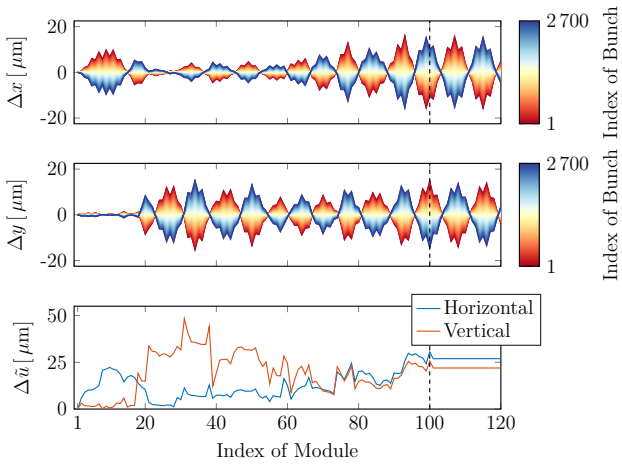

Figure 1: Simulated intra-bunch-train trajectory variation at EuXFEL. The horizontal (up) and vertical (mid) intra-bunch-train offsets are plotted, evaluated at each BPM. The red line corresponds to the first bunch, the blue line to the 2700th bunch of one bunch train. The bottom row shows the normalized trajectory variation. After module 100, a FODO section is appended for visualization purposes.

value which exceeds 90 % of the evaluations and is marked as circles in Fig. 2. It's values are $\Delta\tilde{x}_c = 63\,\mu\text{m}$ and $\Delta\tilde{y}_c = 41\,\mu\text{m}$ for the horizontal and vertical plane, respectively, in L1, $\Delta\tilde{x}_c = 33\,\mu\text{m}$ and $\Delta\tilde{y}_c = 20\,\mu\text{m}$ in L2 and $\Delta\tilde{x}_c = 13\,\mu\text{m}$ and $\Delta\tilde{y}_c = 9\,\mu\text{m}$ for L3. The decreasing difference between the transverse planes from L1 to L3 points out the decreasing impact of coupler kicks at higher beam energy.

Influence of gradient slopes: The slope of the amplitude of the accelerating field within one bunch train, ΔV, is key in the creation of trajectory variations. For typical machine operation at EuXFEL, the amplitude slope is determined mainly by the interaction of a common loaded quality factor Q_L with dissimilar operational gradients of the cavities [12]. LLRF simulations show that these beam loading induced amplitude slopes are proportional to the beam current and can reach up to $4\,\text{MV}\,\text{m}^{-1}$ for the design beam current of 4.5 mA without further Q_L-correction.

The left side of Figure 3 shows the critical trajectory variation $\Delta\tilde{u}_c$ at the end of 100 modules as a function of the

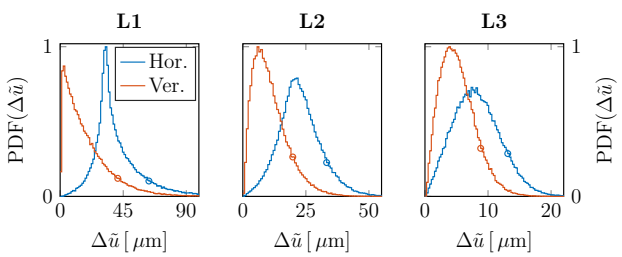

Figure 2: Histogram of the normalized intra-bunch-train trajectory variation $\Delta\tilde{u}$ induced in L1 (left), L2 (mid) and L3 (right) for the horizontal (blue) and vertical (red) plane.

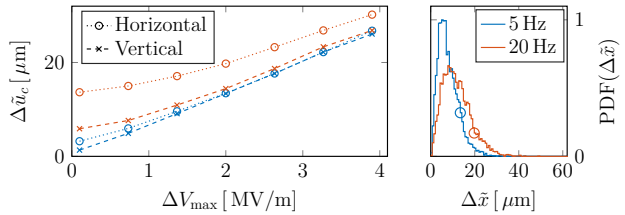

Figure 3: Critical trajectory variation $\Delta\tilde{u}_c$ at the end of L3 as a function of the maximum amplitude slope ΔV_{max} (left) for the horizontal (circles) and vertical (crosses) plane. The two colors correspond to a maximum detuning of $\Delta f = 20\,\text{Hz}$ (red) and $\Delta f = 5\,\text{Hz}$ (blue). The right plot shows the histogram of the horizontal trajectory variation for $\Delta V = 2\,\text{MV}\,\text{m}^{-1}$ for both detuning scenarios.

maximum amplitude slope ΔV_{max}, evaluated for both planes and two detuning scenarios. The blue and red color correspond to a maximum detuning of 5 Hz and 20 Hz, respectively. The right plot shows a histogram of the horizontal trajectory variation for both detuning scenarios. For small detuning and high amplitude slope the trajectory variation is proportional to the amplitude slope and the influence of coupler kicks vanishes. For high beam currents, a limitation of beam loading induced amplitude slopes by changing the Q_L-setup is advised.

Influence of the beam trajectory: In this section two methods for minimizing the intra-bunch-train trajectory variation for a given machine realization are discussed. The effect of a misaligned structure on the trajectory variation depends on the beam trajectory through the structure and the phase advance between individual perturbations. At first, the phase advance is studied. The strength of the horizontally focussing and defocusing quadrupole, k_F and k_D, can be set independently from each other. It is therefore possible to vary the horizontal and vertical phase advance in the accelerating sections independently. For reasons of simplicity only periodic solutions are assumed, meaning that all k_F and k_D, respectively, have the same strength.

Figure 4 shows exemplarily tracking results at the end of a string containing 100 modules for one machine realization, thus RF- and misalignment seed. The accumulated normalized trajectory variation $\Delta\tilde{u}$ is plotted for both transverse planes. The upper two plots show a contour of $\Delta\tilde{x}$ (left) and $\Delta\tilde{y}$ (right) as a function of the horizontal and vertical phase advance, μ_x and μ_y, respectively. The lower plot shows $\Delta\tilde{x}$ and $\Delta\tilde{y}$, evaluated at phase advances which correspond to the dashed line in the upper plots. Obviously individual perturbations cancel remarkably at a certain phase advance while they add up in other cases. This result can be used to improve the multi-bunch performance of the XFEL. During setup of the machine the dependence of the intra-bunch-train trajectory variation on the phase advance can be scanned.

Changing the quadrupole magnets linearly in a way that $k_F + k_D = const$, the whole range of phase advance in both planes can be covered (cf. the dashed line in Figure 4) and

ISBN: 978-3-95450-179-3 doi:10.18429/JACoW-FEL2017-TUP002

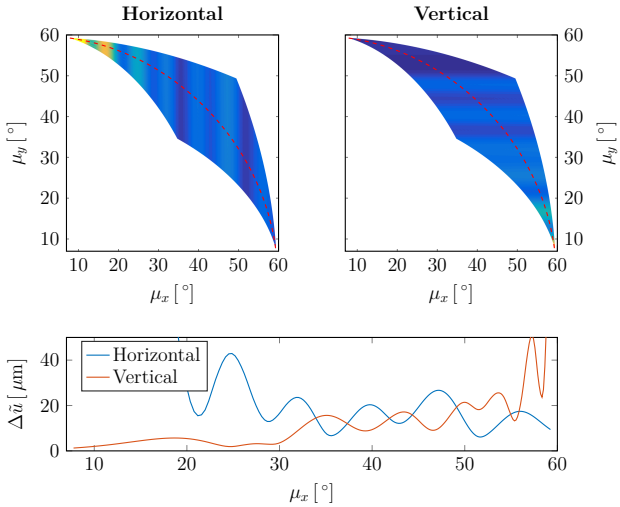

Figure 4: Impact of the phase advance in the FODO-lattice on the accumulated normalized intra-bunch-train trajectory variation $\Delta\tilde{u}$. The upper plots illustrate qualitatively the horizontal (left) and vertical (right) plane as a function of the horizontal and vertical phase advance, μ_x and μ_y, respectively. Bright yellow corresponds to 110 µm and dark blue to 0 µm. The lower plot shows $\Delta\tilde{u}$ evaluated at phase-advances according to the dashed line in the upper plots.

an optimal working point can be chosen. In order to quantify the reduction for any given realization of misalignments and RF parameters, 10^4 machine seeds are randomly created. For each seed, the strength of the quadrupoles is varied and the pair of phase advances is found at which the mean trajectory variation $\langle\Delta\tilde{u}\rangle$, averaged over both transverse planes, is minimized. The range of k-values is $k_i \in [0.05, 0.07]$.

Figure 5 illustrates the results. The black histogram in the left plot shows the distribution of $\langle\Delta\tilde{u}\rangle$ as calculated for $k_F = k_D = 0.065\,\mathrm{m}^{-}2$. This corresponds to a phase advance of about 45° in both planes and reflects the design lattice. The blue line corresponds to the distribution of tracking results with a tune that minimizes $\langle\Delta\tilde{u}\rangle$. The right histogram shows the relative amount of trajectory variation reduction. For most machine realizations the intra-bunch-train trajectory variation can be decreased significantly. In average, a reduction of 73 % is possible. In 90 % of the cases the achievable reduction is larger than 49 %. Note that a reduction of 66 % reflects a final trajectory variation three times smaller than its initial value.

So far, the beam entered the first accelerating module on axis. The impact of a variation of the initial beam trajectory on the accumulated intra-bunch-train trajectory variation is considered in the following. This scenario reflects steering the beam at the entrance of L1. Note that no initial intra-bunch-train trajectory variation and only one pair of steerers are considered. 10^4 machine realizations are evaluated. Analog to the previous method, the beam trajectory angle at the entrance of the first module is changed for each machine seed. The pair of horizontal and vertical trajectory angles

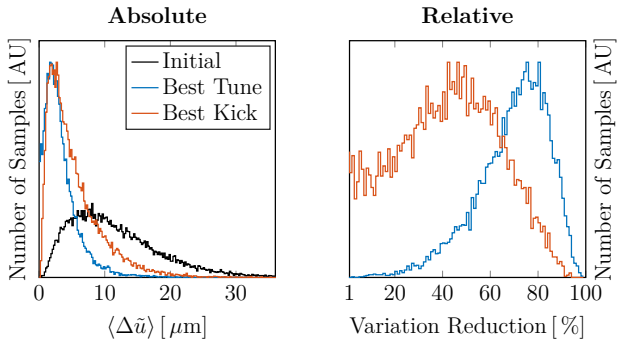

Figure 5: Absolute (left) and relative (right) reduction of normalized intra-bunch-train trajectory variation $\langle\Delta\tilde{u}\rangle$, averaged over both transverse planes. The black histogram in the left plot reflects the distribution as calculated for the design values. The blue curve corresponds to the remaining trajectory variation after choosing an optimal phase advance. The red curve corresponds to the remaining trajectory variation after choosing an optimal trajectory angle at the entrance of the first module. The right plot shows the relative trajectory variation reduction of both methods.

is found at which the mean accumulated trajectory variation $\langle\Delta\tilde{u}\rangle$ is minimized. The considered range of trajectory angles is ±3 mrad. The results are shown in Fig. 5 in red. In average, a reduction of 44 % is possible. In 90 % of the cases the achievable reduction is larger than 11 %. The rms value of the trajectory angle with best reduction is 1 mrad. The reduction is less noticeable than by changing the optical functions. However, steering the beam is significantly less time-consuming. Note that in this simplified example only one pair of steerers at the entrance of the first module was considered. An automated optimizer including several steerers throughout the accelerator should be implemented and run by default when setting up the machine.

CONCLUSION

Intra-bunch-train trajectory variations which are caused by a variation of RF parameters of individual cavities within one bunch train at EuXFEL have been analyzed systematically. Different accelerating sections and ranges of machine parameter were discussed and methods for reducing the accumulated trajectory variation for a given machine realization were presented. Future studies on limiting the variation of RF parameters by means of a Q_L-correction are advised.

ACKNOWLEDGMENTS

We would like to thank Martin Dohlus, Klaus Flöttman and Julien Branlard for their help in valuable discussions.

REFERENCES

[1] M. Altarelli *et al.*, "XFEL: The European X-Ray Free-Electron Laser - Technical Design Report", DESY-06-097, July 2006.

ISBN: 978-3-95450-179-3 doi:10.18429/JACoW-FEL2017-TUP002

[2] Winfried Decking and Torsten Limberg, "European XFEL Post-TDR Description", Technical Report XFEL.EU TN-2013-004, 2013.

[3] T. Tschentscher. "Layout of the X-Ray Systems at the European XFEL", Technical Report XFEL.EU TR-2011-001, 2011.

[4] M. Bousonville *et al.*, "Planning and Controlling of the Cold Accelerator Sections Installation in XFEL", in *Proceedings of IPAC'16*, Busan, Korea, 2016, pages 716–718, paper MOPOW006.

[5] B. Aune *et al.*, "Superconducting TESLA cavities", *Phys. Rev. ST Accel. Beams*, 3:092001, Sep 2000.

[6] B. Keil *et al.*, "Design of an Intra-Bunch-Train Feedback System for the European X-Ray FEL", in *Proceedings of DIPAC'07*, Venice, Italy, May 2007, paper WEPB02.

[7] B. Keil *et al.*, "Status of The European XFEL Transverse Intra Bunch Train Feedback System", in *Proceedings of IBIC'15*, Melbourne, Australia, 2015, paper TUPB064.

[8] D. Reschke, V. Gubarev, J. Schaffran, L. Steder, N. Walker, M. Wenskat, and L. Monaco, "Performance in the vertical test of the 832 nine-cell 1.3 GHz cavities for the european x-ray free electron laser", *Phys. Rev. Accel. Beams*, 20:042004, Apr 2017.

[9] T. Schilcher, "Vector Sum control of pulsed accelerating fields in Lorentz Force Detuned Superconducting Cavities", PhD thesis, University of Hamburg, 1998.

[10] J. Branlard *et al.*, "The European XFEL LLRF System", in *Proceedings of IPAC'12*, New Orleans, USA, 2012, page 55, paper MOOAC01.

[11] M. Omet *et al.*, "Operation Experiences with the MICROTCA.4-based LLRF Control System at FLASH", in *Proceedings of IPAC'15*, Richmond, Virginia, USA, 2015, page 844, paper MOPHA029.

[12] T. Hellert, "Intra-Bunch-Train Transverse Dynamics in the Superconducting Accelerators FLASH and European XFEL", PhD thesis, University of Hamburg, 2017.

[13] J. Rosenzweig and L. Serafini, "Transverse particle motion in radio-frequency linear accelerators" *Phys. Rev.* E, 49:1599–1602, Feb 1994.

[14] M. Dohlus, I. Zagorodnov, E. Gjonaj, and T. Weiland, "Coupler Kick for Very Short Bunches and its Compensation", in *Proceedings of EPAC'08*, Genoa, Italy, 2008, page 582, paper MOPP013, JACoW.